

## ORIGINAL ARTICLE

# MBD2 mediates renal cell apoptosis via activation of Tox4 during rhabdomyolysis-induced acute kidney injury

Tianshi Sun<sup>1,2,3</sup> | Qing Liu<sup>1</sup> | Yifan Wang<sup>2,3</sup> | Youwen Deng<sup>1</sup>  | Dongshan Zhang<sup>2,3,4</sup>

<sup>1</sup>Department of Spine Surgery, The Third Xiangya Hospital of Central South University, Changsha, China

<sup>2</sup>Department of Emergency Medicine, Second Xiangya Hospital of Central South University, Changsha, China

<sup>3</sup>Emergency Medicine and Difficult Diseases Institute, Second Xiangya Hospital of Central South University, Changsha, China

<sup>4</sup>Department of Nephrology, Second Xiangya Hospital of Central South University, Changsha, China

## Correspondence

Youwen Deng, Department of Spine Surgery, The Third Xiangya Hospital, Central South University, No. 138, Tongzipo Road, Changsha, Hunan 410013, China.  
Email: drywdeng@csu.edu.cn

Dongshan Zhang, Department of Emergency Medicine and Difficult Diseases Institute, Department of Nephrology, Second Xiangya Hospital, Central South University, Changsha, Hunan 410011, China.  
Emails: zhkidney@qq.com; dongshanzhang@csu.edu.cn

## Funding information

National Natural Science Foundation of China, Grant/Award Number: 81472058; Hunan Science and Technology Innovation Plan, Grant/Award Number: 2018SK2105

## Abstract

Our study investigated the role of Methyl-CpG-binding domain protein 2 (MBD2) in RM-induced acute kidney injury (AKI) both in vitro and in vivo. MBD2 was induced by myoglobin in BUMPT cells and by glycerol in mice. MBD2 inhibition via MBD2 small interfering RNA and MBD2-knockout (KO) attenuated RM-induced AKI and renal cell apoptosis. The expression of TOX high mobility group box family member 4 (Tox4) induced by myoglobin was markedly reduced in MBD2-KO mice. Chromatin immunoprecipitation analysis indicated that MBD2 directly bound to CpG islands in the Tox4 promoter region, thus preventing promoter methylation. Furthermore, siRNA inhibition of Tox4 attenuated myoglobin-induced apoptosis in BUMPT cells. Finally, MBD2-KO mice exhibited glycerol-induced renal cell apoptosis by inactivation of Tox4. Altogether, our results suggested that MBD2 plays a role in RM-induced AKI via the activation of Tox4 and represents a potential target for treatment of RM-associated AKI.

## KEYWORDS

AKI, apoptosis, MBD2, rhabdomyolysis, Tox4

## 1 | INTRODUCTION

Rhabdomyolysis (RM) is a life-threatening condition, characterized by skeletal muscle tissue damage and leakage of intracellular components into the bloodstream. Traumatic RM occurs in the case of crush syndrome,<sup>1,2</sup> which is a medical condition that occurs due to crushing skeletal injury in victims of natural disasters (eg earthquakes), accidents and wars.<sup>3,4</sup> One of the most common

complications of RM is acute kidney injury (AKI), and 10% of all AKI patients present with RM.<sup>5</sup> AKI is a clinical disorder with high mortality rates.<sup>6</sup> It is known that the renal toxicity of myoglobin plays a crucial role in RM-induced AKI via increased oxidative stress, cast formation, inflammation and apoptosis.<sup>7</sup> Although numerous studies have focused on RM-induced AKI,<sup>7-10</sup> the underlying mechanisms remain largely unknown, thus resulting in non-specific therapy.

This is an open access article under the terms of the Creative Commons Attribution License, which permits use, distribution and reproduction in any medium, provided the original work is properly cited.

© 2021 The Authors. *Journal of Cellular and Molecular Medicine* published by Foundation for Cellular and Molecular Medicine and John Wiley & Sons Ltd.

Previous research has shown that DNA methylation occurs in regions containing a high density of CpG dinucleotides, which is typically thought to result in epigenetic modification related to transcriptional repression; however, the role and traditional interpretation of DNA methylation has been recently challenged.<sup>11</sup> Based on different methylation patterns, it has been reported that DNA methylation may play a role in both transcriptional activation and silencing. Furthermore, accumulating evidence suggests that DNA methylation is associated with AKI.<sup>5,12,13</sup> However, the role of DNA methylation in RM-induced AKI may vary based on differential regulation of methylation and the type of experimental model used. In mice that are injected with glycerol in their bilateral hindlimb muscles,<sup>14</sup> RM-induced AKI is characterized by renal cortical necrosis, cast formation and inflammatory infiltration.<sup>15,16</sup> Apoptosis is a key phenomenon in glycerol-induced AKI, which may, in turn, be regulated by other cellular pathways.<sup>16-18</sup> Therefore, it is important to gain a holistic understanding of the mechanisms underlying RM-induced AKI to better design targeted treatment therapies.

Here, we aimed to study the role of DNA methylation in AKI by analysing the function of Methyl-CpG-binding domain protein 2 (MBD2), a key methylated protein reader, in RM-induced AKI, both *in vitro* using a mouse proximal tubule-derived cell line (BUMPT) and *in vivo* using C57BL/6 mice.

## 2 | MATERIALS AND METHODS

### 2.1 | Reagents and antibodies

Antibodies were purchased from the following sources: MBD2 from Abcam (Cambridge, UK);  $\beta$ -Tubulin from Santa Cruz Biotechnology (Santa Cruz, CA, USA); Caspase-3, cleaved caspase-3 from Cell Signaling Technology (Danvers, MA, USA); Tox4 (PA5-53653) from Thermo Fisher Scientific (Waltham, MA, USA). Myoglobin and ascorbic acid were purchased from Sigma-Aldrich (St. Louis, MO, USA). The Tox4 promoter containing the methylated target sequences of MBD2 was subcloned into a CpG-free pCpG luciferase reporter vector (Invitrogen Biotechnology, Shanghai, China). Construction of methylation promoter of Tox4 CpG-free pCpG luciferase reporter, MBD2 and mtMBD2 (the deletion of the methylated DNA-binding domain) plasmids as described previously.<sup>36,37</sup> Small interfering RNAs (siRNAs) against MBD2 and Tox4 were synthesized by RUIBO Biology Co., Ltd. (Guangdong, Guangzhou, China), as previously described.<sup>26</sup>

### 2.2 | Animal model of RM-induced AKI

MBD2 knockout (MBD2-KO) mice were obtained from Cyagen Biosciences Co., Ltd (Guangzhou, China). Male MBD2-KO mice aged 10-12 weeks were injected in the bilateral hindlimb skeletal muscles with a dose of 8.0 mL/kg glycerol (50% v/v in sterile

saline); the control group was injected with an equal volume of normal saline. Littermate male MBD2-wild-type (WT) mice were treated using the same method mentioned above. Animal experimental protocols were approved by the Care and Use of Laboratory Animals Institutional Committee from Second Xiangya Hospital, China. The mice were housed at stable room temperature in a 12-hour light/dark cycle and provided adequate supplies of standard rodent chow and water.

### 2.3 | Cell culture and treatments

BUMPT cells were cultured in Dulbecco's modified Eagle's medium with 10% foetal bovine serum, 0.5% penicillin (Thermo Fisher Scientific), and streptomycin, and then maintained in a 5%-CO<sub>2</sub> incubator at 37°C. Both myoglobin and ascorbic acid were then added to the medium at a final concentration of 200 mM (3.6 mg/mL) and 2 mM, respectively. Ascorbic acid reduces myoglobin to a ferrous status,<sup>29</sup> and the cytotoxic ferrous myoglobin causes renal tubular injury. Chromatin immunoprecipitation (ChIP) experiments were performed using anti-MBD2, according to the ChIP kit assay procedure (Millipore, Burlington, MA, USA). Immunoprecipitated DNA was amplified by polymerase chain reaction (PCR) using the following primers that bound to CpG islands in the binding of promoter of Tox4 promoter:

F1:5'-GGAGGGTTGGGGTTTTAGTA-3'; R1:5'-AACATCAACA ACTTTTACTCACCTC-3'; F2:5'-GGAGGGTTGGGGTTTTAGTA-3'; R2:5'-CAACATCAACA ACTTTTACTCACCT-3'; F3:5'-GGAGGGTTG GGGTTTTAGTA-3'; R3:5'-CCAACATCAACA ACTTTTACTCAC-3'; F4:5'-GGAGGGTTGGGGTTTTAGTA-3'; R4:5'-ACATCAACA ACTTT TACTCACCTC-3'; F5:5'-GGAGGGTTGGGGTTTTAGTA-3'; R5:5'-CC CAACATCAACA ACTTTTACTC-3.

Transcriptional activation activity of Tox4 was measured using the luciferase kit (Promega, Madison, WI, USA), as described previously.<sup>26,30-31</sup>

### 2.4 | Analysis of apoptosis

Apoptosis in kidney tissues was analysed by terminal deoxynucleotidyl transferase-mediated digoxigenin-deoxyuridine nick-end labelling (TUNEL) assay using the In Situ Cell Death Detection Kit from Roche Diagnostics (Indianapolis, IN). Apoptosis in cell cultures was analysed by flow cytometry (FCM), as previously described.<sup>26,31,35</sup>

### 2.5 | Methylated CpG-DNA immunoprecipitation

Immunoprecipitation of methylated CpG-DNA was performed, as described previously (Zymo Research, Irvine, CA, USA).<sup>32</sup> Briefly, sheared DNA was used for methylated CpG immunoprecipitation, and the methylated DNA was analysed by PCR analysis using an ABI Onestepplus real-time PCR system.

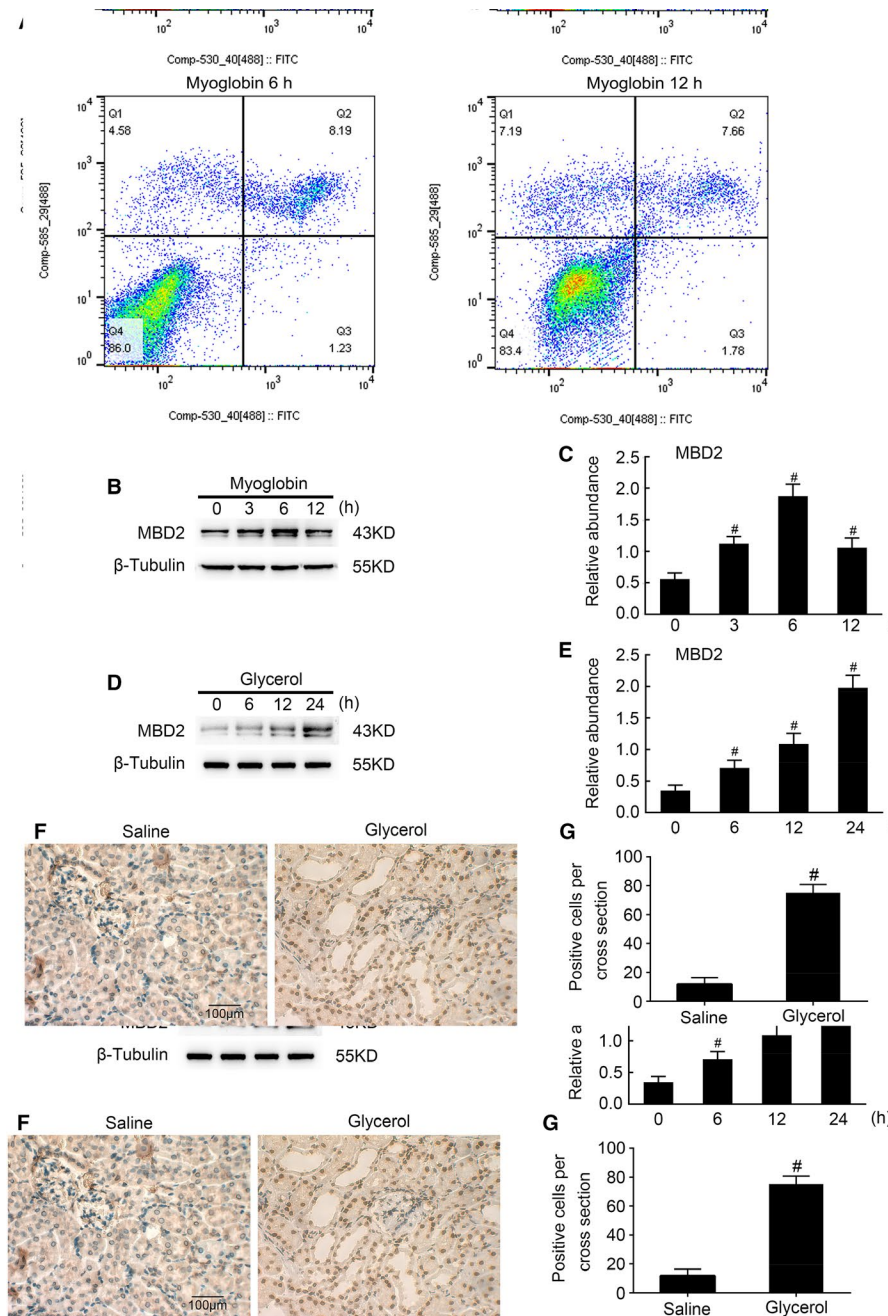


**FIGURE 1** Rhabdomyolysis induced the expression of MBD2 in both BUMPT cells and mice kidneys. BUMPT cells were administered with 3.6 mg/mL ferrous myoglobin and analysed for 0–12 h and male C57BL/6 mice were injected with 8.0 mL/kg glycerol and analysed for 0–24 h, respectively. A, Flow cytometry analysis of apoptosis in myoglobin-treated BUMPT cells. B and D, Whole protein lysates from cells and kidney tissues were gathered for Western blot analysis of MBD2 expression at the indicated time points. C and E, Densitometric ratios of MBD2/ $\beta$ -Tubulin. F and G, Immunohistochemical staining and the calculation of MBD2 expression. Scale bar, 100  $\mu$ M. Data are expressed as mean  $\pm$  SD ( $n = 6$ ). # $P < .05$  vs 0 h group or Saline group. Original magnification, 400 $\times$  in F

## 2.6 | Histology, immunohistochemistry and immunoblot analyses

Haematoxylin and eosin (H&E) staining was used for histological analysis. The tubular damage scores were assessed according to the percentage of damaged tubules, as described previously.<sup>26</sup> TUNEL assay was used for detecting renal cell apoptosis, and the percentage of the total number of TUNEL-positive cells were calculated in 10–20 microscopic fields that were randomly selected per tissue section.<sup>33</sup> Immunohistochemical staining and image analysis of MBD2 were performed according to previously described methods.<sup>34</sup> Lysates of kidney tissues and BUMPT cells

were subjected to sodium dodecyl sulphate-polyacrylamide gel electrophoresis and immunoblotting was performed using MBD2, Tox4, Caspase-3, cleaved caspase-3 and  $\beta$ -Tubulin antibodies following standard procedures.

## 2.7 | Statistical analysis

Data were expressed as mean  $\pm$  standard deviation (SD). Two-group comparisons were made using 2-tailed Student *t* tests. Multiple group data were evaluated using one-way analysis of variance.  $P < .05$  was considered statistically significant.

### 3 | RESULTS

#### 3.1 | MBD2 expression was induced by RM in BUMPT cells and C57BL/6 mice

Using Western blotting, we investigated the expression of MBD2 induced by RM-associated AKI at different time points in BUMPT cells treated with ferrous myoglobin and renal tissues of C57BL/6 mice injected with glycerol. The flow cytometry analysis showed that myoglobin induced the BUMPT cell apoptosis. As shown in Figure 1B-E, MBD2 expression levels gradually increased in BUMPT cells and renal tissues over time compared with baseline. Interestingly, *in vitro* MBD2 expression peaked at the 6 hours time point (Figure 1A,B). Although MBD2 levels decreased thereafter, they remained higher than pre-treatment levels at 12 hours after myoglobin treatment. Furthermore, immunohistochemical analysis of the renal tissues of C57BL/6 mice injected with glycerol confirmed that MBD2 expression was mainly localized in the tubular cell nuclei (Figure 1F,G). Altogether, the results indicated that MBD2 expression levels were up-regulated both *in vitro* and *in vivo* during RM-associated AKI.

#### 3.2 | Renal dysfunction, tubular damage and cell apoptosis are attenuated in MBD2-KO mice during RM-induced AKI

We injected the MBD2-KO and WT littermate mice with glycerol and analysed the effects after 24 hours. Glycerol injections induced renal failure in WT mice, as indicated by the increased levels of blood urea nitrogen (BUN) and creatinine compared with control. However, in MBD2-KO mice, the increase in BUN and creatinine levels was lower compared with that in MBD2-WT mice (Figure 2A,B). H&E staining also confirmed that the deletion of MBD2 markedly reduced tubular damage in the cortex of the kidney in glycerol-injected mice (Figure 2C). Additionally, glycerol-injected MBD2-KO mice showed a lower tubular damage score of 1.9 compared with glycerol-injected WT mice that showed a score of 3.5 (Figure 2D). Previous results have indicated that apoptosis plays a key role in the progression of RM-induced AKI.<sup>16,17,19-21</sup> To investigate whether MBD2 promoted renal cell apoptosis and, therefore, tubular cell damage, we performed TUNEL staining to assess apoptosis in WT and MBD2-KO renal tissues. We observed increased apoptosis in the kidney cells of glycerol-injected WT mice compared with those of MBD2-KO mice (Figure 2E), and this increase was also reflected by the increased number of TUNEL-positive cells in WT mice compared with MBD2-KO mice (Figure 2F). Moreover, Western blotting showed that the levels of cleaved caspase-3 were markedly lower in MBD2-KO cells than in WT cells (Figure 2G), which was also supported by densitometric quantitation (Figure 2H).

#### 3.3 | MBD2 mediated myoglobin-induced apoptosis in BUMPT cells

As MBD2 expression was up-regulated as a result of myoglobin treatment in BUMPT cells (Figure 1A,B), we investigated whether MBD2 played a role in renal cell apoptosis *in vitro*. BUMPT cells were first transfected with MBD2 siRNA or MBD2-containing plasmid, followed by myoglobin or saline treatment. Flow cytometry analysis demonstrated that the transfection of MBD2 siRNA reduced apoptosis in BUMPT cells induced by myoglobin (Figure 3A). Immunoblotting analysis showed that MBD2 siRNA markedly down-regulated the expression levels of MBD2 and cleaved caspase-3 (Figure 3B), which was confirmed by densitometric analysis (Figure 3C). In contrast, myoglobin-treated BUMPT cells containing the MBD2 plasmid showed increased levels of cleaved caspase-3 compared with those cells that lacked the plasmid (Figure 3D), indicating that apoptosis was enhanced in myoglobin-treated cells that ectopically expressed MBD2. This result was further validated by immunoblotting and densitometric analyses (Figure 3E,F).

#### 3.4 | Tox4 is down-regulated in MBD2-KO mice and is involved in renal cell apoptosis

*Tox4* is novel gene that is reportedly involved in DNA reprogramming, transcription modulation and apoptosis,<sup>22-24</sup> we investigated whether *Tox4* was involved in renal cell apoptosis and if MBD2 played a role in *Tox4* regulation during glycerol-induced AKI. First, we checked *Tox4* expression levels in mice during glycerol-induced AKI. As shown in Figure 4A, *Tox4* expression gradually increased over time in WT mouse kidney tissues up to 24 hours after glycerol injection, which was verified by densitometric quantitation (Figure 4B). Real-time PCR analysis showed that *Tox4* expression was up-regulated in WT mice compared with MBD2-KO mice during RM-induced AKI (Figure 4C), which was confirmed by Western blotting and densitometric analyses (Figure 4D,E). Interestingly, addition of *Tox4* siRNA suppressed apoptosis in myoglobin-treated BUMPT cells (Figure 4F). These results were also verified by Western blotting, which showed a down-regulation of cleaved caspase-3 in myoglobin-treated BUMPT cells transfected with *Tox4* siRNA compared with control (Figure 4G). Densitometric analysis confirmed the results of western blotting (Figure 4H). Altogether, the results indicated that MBD2 KO resulted in reduced expression of *Tox4* *in vivo* compared with WT; and inactivation of *Tox4* attenuated BUMPT cell apoptosis *in vitro*.

#### 3.5 | MBD2 up-regulates Tox4 expression by inhibiting methylation of the Tox4 promoter

We next investigated whether MBD2 regulated *Tox4* expression via DNA methylation. *Tox4* has been predicted by MethPrimer to contain

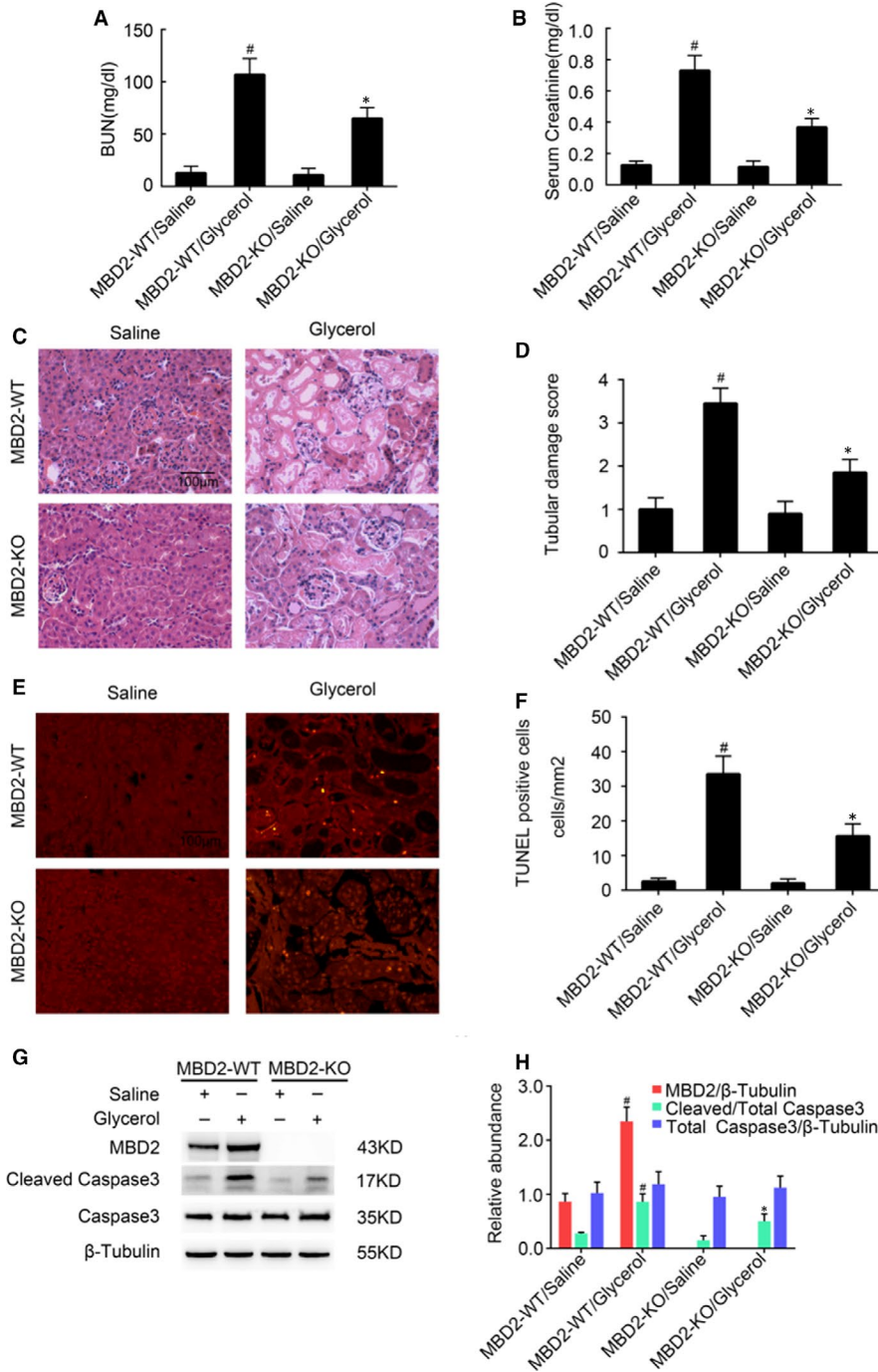
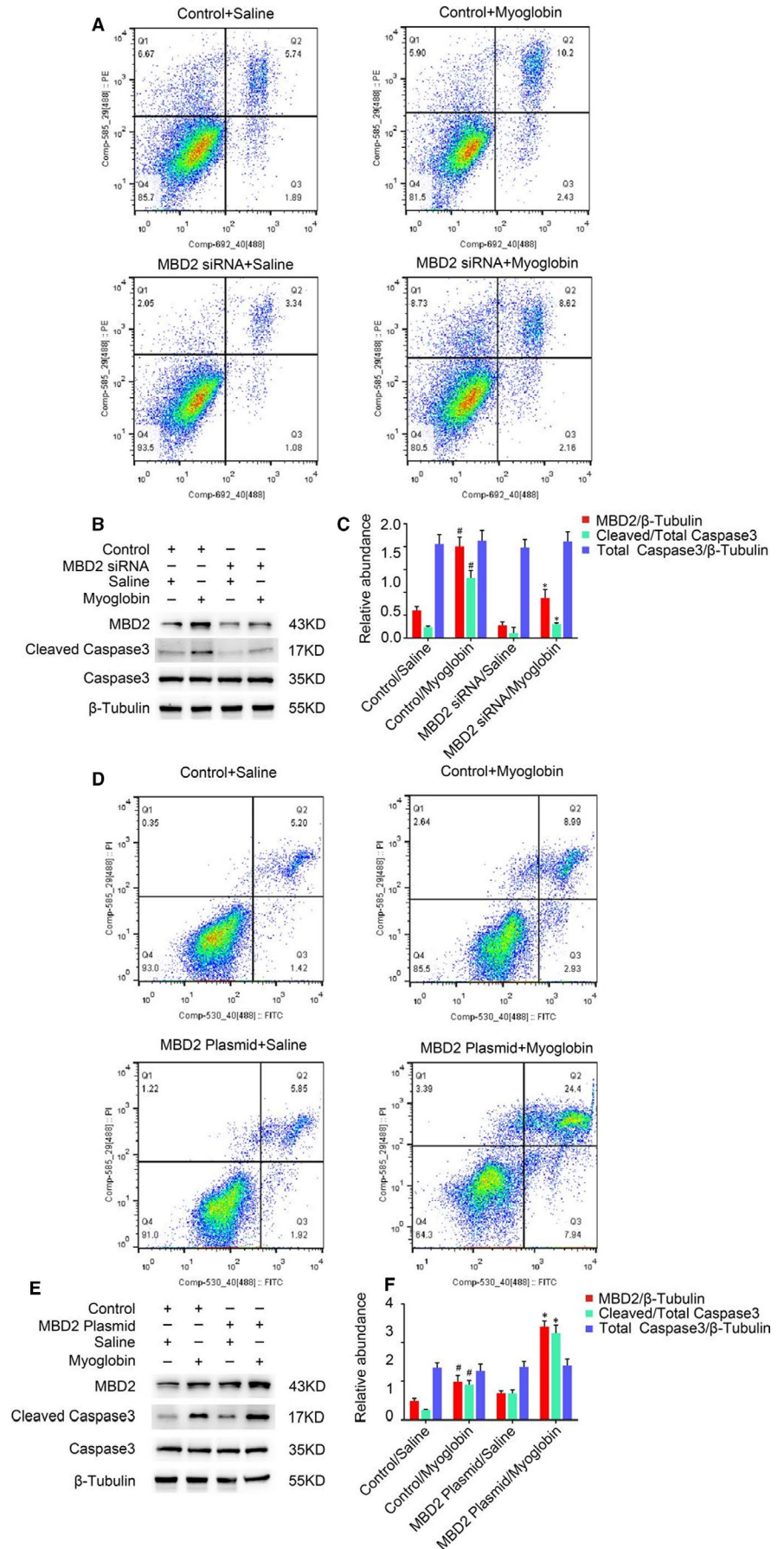


**FIGURE 2** Amelioration of glycerol-induced acute kidney injury and renal cell apoptosis in MBD2-knockout (KO) mice. The MBD2-KO and wild-type (WT) littermate mice were injected with 8.0 mL/kg glycerol or saline as control for 24 h. A and B, Serum creatinine and blood urea nitrogen (BUN) were used for assessing renal function. C, The renal tissue sections were stained with haematoxylin & eosin (H&E). D, Tubular damage score in glycerol-treated kidney cortical tissues. E, Apoptosis was analysed using the TUNEL assay. F, The calculation of TUNEL-positive cells. G, Western blot analysis of MBD2, Caspase-3, cleaved caspase-3, and β-Tubulin expression. H, Densitometric ratios of MBD2, Caspase-3, cleaved caspase-3 and β-Tubulin. Scale bar, 100 μm. Data are expressed as mean ± SD (n = 6). <sup>#</sup>P < .05 vs Saline group, <sup>\*</sup>P < .05 vs MBD2-WT/glycerol group. Original magnification, 400× in A and 200× in E

a CpG island in its promoter region (<http://www.urogene.org/cgi-bin/methprimer/MethPrimer.cgi>), and five pairs of PCR primers for this region have been designed by this website (Figure 5A). ChIP assays showed two binding sites for MBD2 in the *Tox4* promoter region—a 160-bp fragment (mBS1) and a 161-bp fragment (mBS2) (Figure 5B), which validated the prediction that MBD2 could directly bind to the *Tox4* promoter region. The *Tox4* promoter region containing the DNA methylation target sequences was cloned into a CpG-free pCpG luciferase reporter plasmid and co-transfected with plasmids containing MBD2 or mutated MBD2 that lacks the DNA-binding domain (mtMBD2) into BUMPT cells. We found that the MBD2 plasmid

markedly activated the transcription level of *Tox4* compared with the plasmid containing mtMBD2 and the control plasmid (Figure 5C). Methylation analysis indicated that endogenous MBD2-bound DNA markedly suppressed the methylated *Tox4* pCpG; meanwhile, this suppression impact was significantly increased by ectopic MBD2 (Figure 5D). Immunoblot analysis showed that *Tox4* expression was up-regulated by the addition of myoglobin, which was further enhanced by ectopic MBD2 expression (Figure 5G,H). In contrast, MBD2 siRNA treatment suppressed the myoglobin-induced up-regulation of *Tox4* (Figure 5E,F). Altogether, the results demonstrated that MBD2 enhanced the expression level of *Tox4* via promoter demethylation.

**FIGURE 3** MBD2 mediated myoglobin-induced renal cell apoptosis in BUMPT cells. BUMPT cells were transfected with 50 nmol/L MBD2 plasmid or MBD2 siRNA, followed by treatment with 200 mM ferrous myoglobin for 6 h. A and D, Flow cytometry analysis of apoptosis in myoglobin-treated BUMPT cells. B and E, Western blot of MBD2, Caspase-3, cleaved caspase-3, and  $\beta$ -Tubulin expression. C and F, Protein expression levels were quantified by densitometry. Data are expressed as mean  $\pm$  SD ( $n = 6$ ). # $P < .05$  vs Control/Saline group, \* $P < .05$  vs Control/Myoglobin group



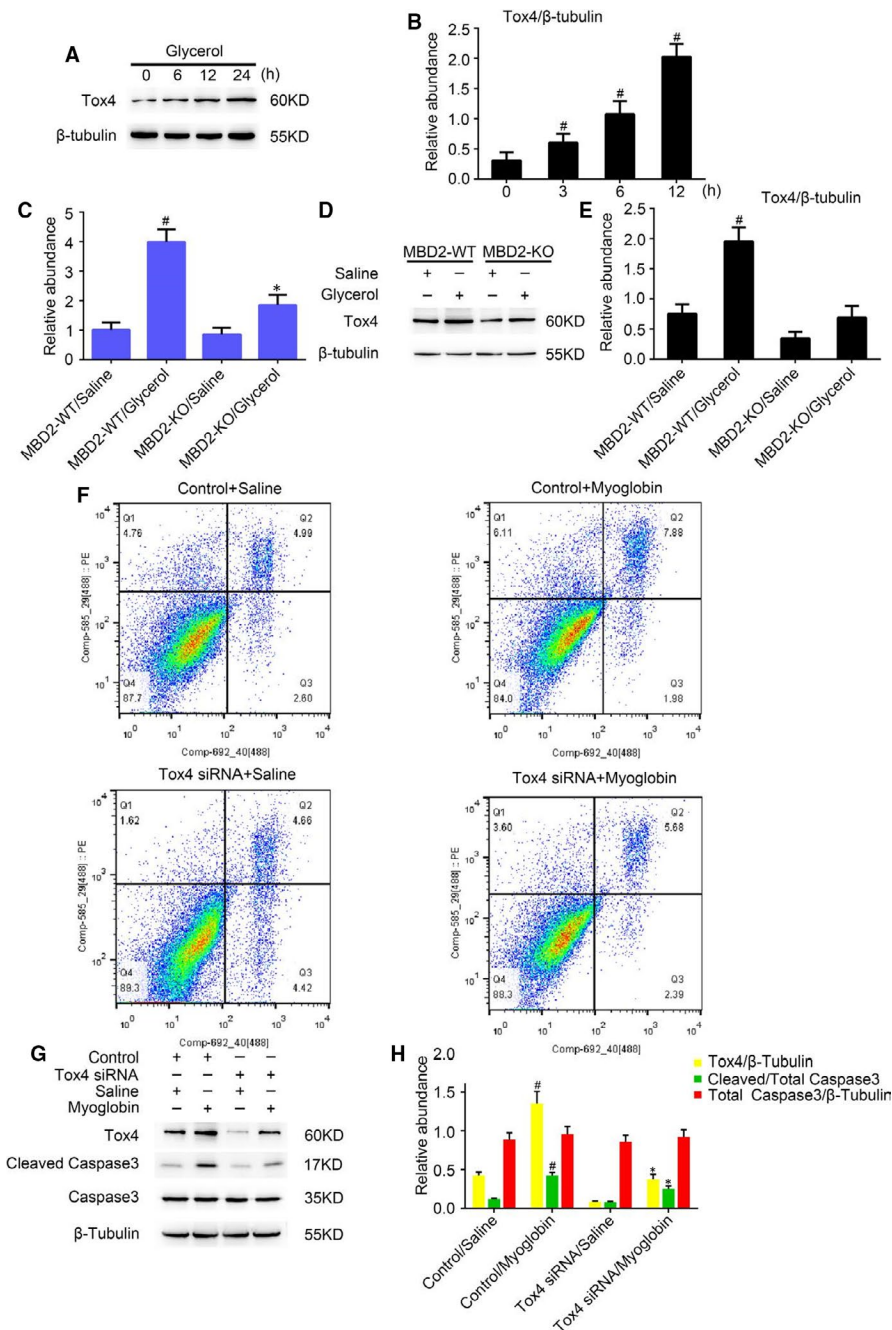


**FIGURE 4** Tox4 expression is inhibited in MBD2-knockout (KO) mice during RM-induced AKI, and Tox4 mediated renal cell apoptosis in myoglobin-treated BUMPT cells. Wild-type (WT) and MBD2-KO littermate mice were injected with 8.0 mL/kg glycerol or saline as control and assessed for 24 h. A, Western blot analysis of Tox4 and β-Tubulin expression over time. B, Densitometric ratios of Tox4/β-Tubulin over time. C, Real-time PCR analysis of Tox4 expression. D, Expression levels of Tox4 and β-Tubulin tested by western blotting in WT and MBD2-KO mice with and without glycerol treatment. E, Densitometric ratios of Tox4/β-Tubulin WT and MBD2-KO mice with and without glycerol treatment. F, Flow cytometry analysis of apoptosis in myoglobin-treated BUMPT cells. G, Western blot of MBD2, Caspase-3, cleaved caspase-3 and β-Tubulin expression. H, Protein expression levels were quantified by densitometry. Data are expressed as mean ± SD (n = 6). #P < .05 vs MBD2-WT/Saline group, \*P < .05 vs MBD2-WT/glycerol group in B, C and E. #P < .05 vs Control/Saline group, \*P < .05 vs Control/Myoglobin group in G

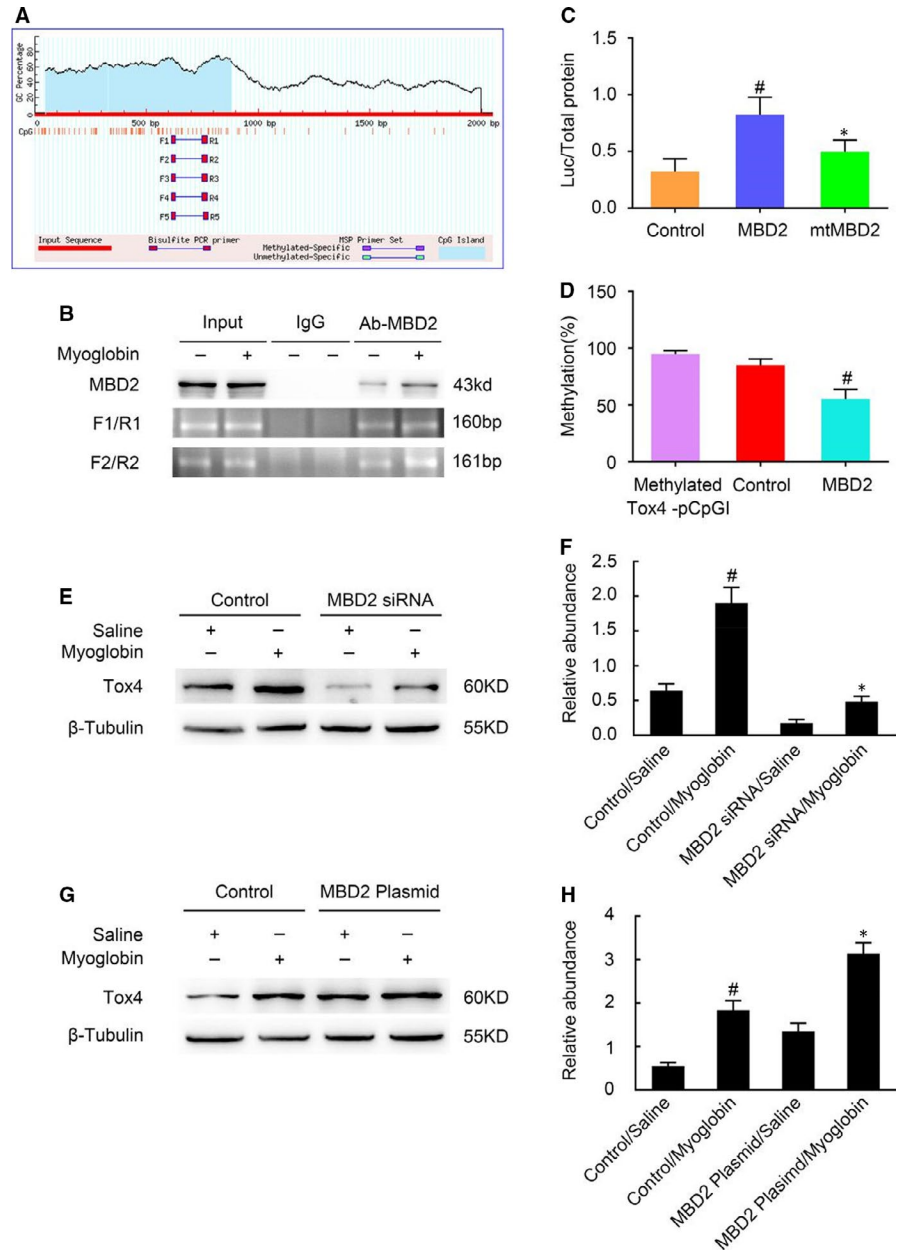
## 4 | DISCUSSION

RM is often accompanied by AKI caused by crushing trauma.<sup>5,25</sup> However, due to a lack of knowledge of the underlying mechanisms, no specific therapies for RM-induced AKI currently exist, thus making it a life-threatening medical condition. We believe that the present study is the first to show that MBD2 induces renal cell apoptosis in RM-induced AKI by up-regulating Tox4 expression via promoter demethylation.

We have previously shown that MBD2 mediates apoptosis during vancomycin-associated AKI.<sup>26</sup> In this study, we observed that MBD2 is activated by glycerol in mice and by myoglobin in BUMPT cells, and its expression is largely localized in the nucleus of injured tubular cells

(Figure 1). Our results also showed that the deletion of MBD2 could attenuate renal injury and dysfunction in RM-induced AKI mice. Previous results have indicated that apoptosis plays a key role in the progression of RM-induced AKI.<sup>16,17,19-21,27</sup> However, few researches have revealed the connection and the underlying mechanism between apoptosis and DNA methylation.<sup>28</sup> MBD2, a key methylated protein reader, is known to have unique functions that have been shown to contribute to transcriptional regulation in pluripotent cells, immune lymphocytes and in tumorigenesis. Therefore, experiments were carried out and the results showed that glycerol-induced renal cell apoptosis was significantly attenuated in MBD2-KO mice in vivo, and myoglobin-induced BUMPT cell apoptosis was reduced by MBD2 siRNA treatment in vitro, thus indicating an important role for MBD2 in renal cell apoptosis.

**FIGURE 5** MBD2 directly binds to CpG islands in the promoter of *Tox4* and positively activates transcription via demethylation. A, the presence of CpG islands in the *Tox4* promoter and five pairs of primer sequences were predicted by the MethPrimer software. B, Chromatin isolated from BUMPT cells treated with or without myoglobin were used for ChIP assays, which revealed MBD2-binding sites on the *Tox4* promoter. C, Relative luciferase activity of the MBD2 or MBD2 lacking the methylated DNA-binding domain (mtMBD2) plasmids co-transfected with the methylated *Tox4* pCpGI plasmid in BUMPT cells. D, CpG-DNA methylation of the *Tox4* promoter region. E and G, Expression levels of *Tox4* and  $\beta$ -Tubulin detected by immunoblotting. F and H, Greyscale image analysis of *Tox4* levels normalized to  $\beta$ -Tubulin levels. These data are shown as means  $\pm$  SD ( $n = 6$ ). # $P < .05$  vs Control/Saline group. \* $P < .05$  vs Control/myoglobin group



The above findings revealed that MBD2 plays a pivotal role in this model; however, the molecular mechanism of this role required further investigation. Therefore, we assessed the changes in downstream gene expression in response to glycerol injection. Both PCR and immunoblot results indicated that the expression level of *Tox4* was increased in WT mice during RM-induced AKI and reduced in MBD2-KO mice (Figure 4A-E). The functional analysis indicated that *Tox4* positively regulated cell apoptosis and the protein expression level of cleaved caspase-3 confirmed this conclusion (Figure 4F-H). Thus, inhibition of *Tox4* ameliorates myoglobin-induced renal cell apoptosis suggesting that *Tox4* may be a potential therapeutic target for RM-associated AKI. We also found that the expression of *Tox4* was up-regulated following transfection of the MBD2 plasmid, whereas it was decreased in response to the MBD2 siRNA treatment (Figure 5E-H). The ChIP assays demonstrated that MBD2 could directly interact with a binding site within the *Tox4* promoter domain

it (Figure 5B). Moreover, observed that MBD2 activated *Tox4* via demethylation (Figure 5C,D). These results confirmed our hypothesis that *Tox4* is a direct downstream target gene of MBD2. In recent studies, *Tox4* was identified as a novel transcriptional modulator,<sup>22</sup> but the impact of *Tox4* on apoptosis in this experimental model remained poorly understood. In order to explore the regulatory mechanism of *Tox4* in RM-associated AKI, we transfected *Tox4* siRNA synthesized by the Ruibo RUIBO Biology company Co. in BUMPT cells. As shown in Figure 6, our results verified that *Tox4* promoter had a direct interaction with MBD2 in this experimental model, which up-regulated *TOX4* transcription level and its protein expression. However, we have not found the interactions between *Tox4* protein and other apoptotic proteins or DNA fragments, which need to be further explored in the future work.

In conclusion, our results indicated that MBD2 mediates apoptosis during RM-associated AKI. In addition, we found that MBD2

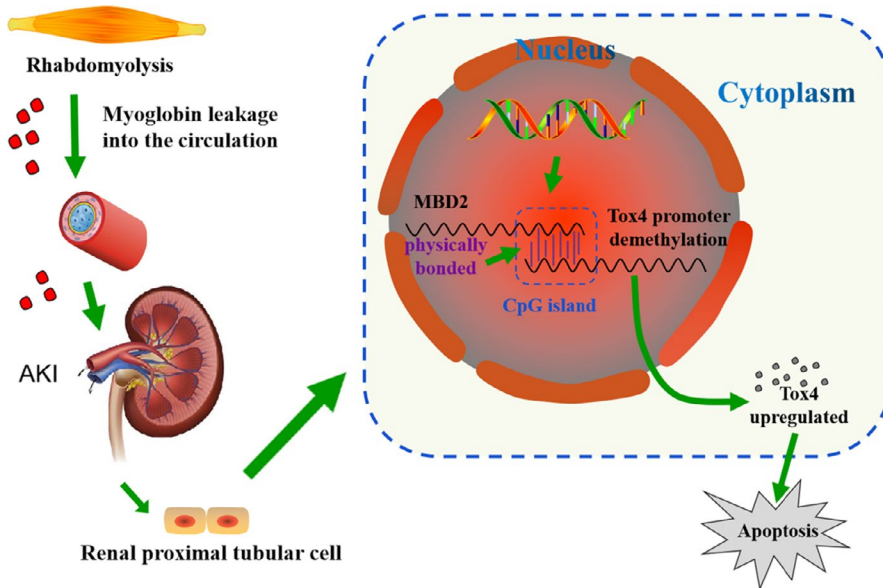


**FIGURE 6** The molecular mechanism of MBD2 in rhabdomyolysis (RM)-associated acute kidney injury (AKI). When RM occurs, myoglobin is released into the blood, thus inducing nephrotoxicity and, often, AKI. Subsequently, MBD2 activates the expression of Tox4 via demethylation of its promoter, which mediates renal cell apoptosis

regulates the expression of Tox4 via promoter demethylation to induce renal cell apoptosis. Therefore, MBD2 may potentially be a new therapeutic target for treating RM-induced AKI.

#### ACKNOWLEDGEMENTS

This study was supported by National Natural Science Foundation of China (No. 81472058), the Hunan Science and Technology Innovation Plan (2018SK2105).

#### CONFLICT OF INTEREST

The authors declare that the research was conducted in the absence of any commercial or financial relationships that could be construed as a potential conflict of interest.

#### AUTHOR CONTRIBUTION

**Tianshi Sun:** Data curation (equal); formal analysis (equal); investigation (equal); methodology (equal); project administration (equal); resources (equal); software (equal); supervision (equal); validation (equal); visualization (equal); writing – original draft (equal); writing – review and editing (equal). **Qing Liu:** Formal analysis (equal); investigation (equal); software (equal); supervision (equal); writing – review and editing (equal). **Yifan Wang:** Investigation (equal); methodology (equal); software (equal). **Youwen Deng:** Conceptualization (equal); funding acquisition (equal); supervision (equal); writing – review and editing (equal). **Dongshan Zhang:** Conceptualization (equal); methodology (equal); resources (equal); writing – review and editing (equal).

#### CONSENT FOR PUBLICATION

Figures in the manuscript have been published with the consent of all the authors.

#### ORCID

Youwen Deng  <https://orcid.org/0000-0002-9117-4078>

#### REFERENCES

- Nance JR, Mammen AL. Diagnostic evaluation of rhabdomyolysis. *Muscle Nerve*. 2015;51:793-810.
- Torres PA, Helmstetter JA, Kaye AM, Kaye AD. Rhabdomyolysis: pathogenesis, diagnosis, and treatment. *Ochsner J*. 2015;15(1):58-69.
- Peiris D. A historical perspective on crush syndrome: the clinical application of its pathogenesis, established by the study of wartime crush injuries. *J Clin Pathol*. 2017;70(4):277-281.
- Sever MS, Vanholder R, Lameire N. Management of crush-related injuries after disasters. *N Engl J Med*. 2006;354(10):1052-1063.
- Belliere J, Casemayou A, Ducasse L, et al. Specific macrophage subtypes influence the progression of rhabdomyolysis-induced kidney injury. *J Am Soc Nephrol*. 2015;26(6):1363-1377.
- Odutayo A, Wong CX, Farkouh M, et al. AKI and long-term risk for cardiovascular events and mortality. *J Am Soc Nephrol*. 2017;28(1):377-387.
- Panizo N, Rubio-Navarro A, Amaro-Villalobos JM, Egido J, Moreno JA. Molecular mechanisms and novel therapeutic approaches to rhabdomyolysis-induced acute kidney injury. *Kidney Blood Press Res*. 2015;40(5):520-532.
- Lee CW, Kou HW, Chou HS, et al. A combination of SOFA score and biomarkers gives a better prediction of septic AKI and in-hospital mortality in critically ill surgical patients: a pilot study. *World J Emerg Surg*. 2018;13:41.
- Okubo K, Kurosawa M, Kamiya M, et al. Macrophage extracellular trap formation promoted by platelet activation is a key mediator of rhabdomyolysis-induced acute kidney injury. *Nat Med*. 2018;24(2):232-238.
- Nishida K, Watanabe H, Ogaki S, et al. Renoprotective effect of long acting thioredoxin by modulating oxidative stress and macrophage migration inhibitory factor against rhabdomyolysis-associated acute kidney injury. *Sci Rep*. 2015;5:14471.
- Wood KH, Zhou Z. Emerging molecular and biological functions of MBD2, a reader of DNA methylation. *Front Genet*. 2016;7:93.
- Mehta TK, Hoque MO, Ugarte R, et al. Quantitative detection of promoter hypermethylation as a biomarker of acute kidney injury during transplantation. *Transplantation Proc*. 2006;38(10):3420-3426.
- Guo C, Pei L, Xiao X, et al. DNA methylation protects against cisplatin-induced kidney injury by regulating specific genes, including interferon regulatory factor 8. *Kidney Int*. 2017;92(5):1194-1205.

14. Zager RA. Marked protection against acute renal and hepatic injury after nitrated myoglobin + tin protoporphyrin administration. *Transl Res.* 2015;166(5):485-501.
15. Alge JL, Arthur JM. Biomarkers of AKI: a review of mechanistic relevance and potential therapeutic implications. *Clin J Am Soc Nephrol.* 2015;10(1):147-155.
16. Geng X, Hong Q, Wang W, et al. Biological membrane-packed mesenchymal stem cells treat acute kidney disease by ameliorating mitochondrial-related apoptosis. *Sci Rep.* 2017;7:41136.
17. Abd-Ellatif RN, Hegab II, Atef MM, Sadek MT, Hafez YM. Diacerein protects against glycerol-induced acute kidney injury: Modulating oxidative stress, inflammation, apoptosis and necroptosis. *Chem Biol Interact.* 2019;306:47-53.
18. Li O, Geng X, Ma Q, et al. Gene microarray integrated with high-throughput proteomics for the discovery of transthyretin in rhabdomyolysis-induced acute kidney injury. *Cell Physiol Biochem.* 2017;43(4):1673-1688.
19. Feng Y, Huang R, Guo F, et al. Selective histone deacetylase 6 inhibitor 23BB alleviated rhabdomyolysis-induced acute kidney injury by regulating endoplasmic reticulum stress and apoptosis. *Front Pharmacol.* 2018;9:274.
20. Uchida A, Kidokoro K, Sogawa Y, et al. 5-Aminolevulinic acid exerts renoprotective effect via Nrf2 activation in murine rhabdomyolysis-induced acute kidney injury. *Nephrology.* 2019;24(1):28-38.
21. Yin M, Jiang N, Guo L, et al. Oleuropein suppresses oxidative, inflammatory, and apoptotic responses following glycerol-induced acute kidney injury in rats. *Life Sci.* 2019;232:116634.
22. Vanheer L, Song J, De Geest N, et al. Tox4 modulates cell fate reprogramming. *J Cell Sci.* 2019;132(20):jcs232223.
23. Morand B, du Puch C, Barbier E, et al. TOX4 and its binding partners recognize DNA adducts generated by platinum anticancer drugs. *Arch Biochem Biophys.* 2011;507(2):296-303.
24. Morchikh M, Naughtin M, Di Nunzio F, et al. TOX4 and NOVA1 proteins are partners of the LEDGF PWWP domain and affect HIV-1 replication. *PLoS One.* 2013;8(11):e81217.
25. Cabral BMI, Edding SN, Portocarrero JP, Lerma EV. Rhabdomyolysis. *Dis Mon.* 2020;66(8):101015.
26. Wang J, Li H, Qiu S, Dong Z, Xiang X, Zhang D. MBD2 upregulates miR-301a-5p to induce kidney cell apoptosis during vancomycin-induced AKI. *Cell Death Dis.* 2017;8(10):e3120.
27. Tang WX, Wu WH, Qiu HY, Bo H, Huang SM. Amelioration of rhabdomyolysis-induced renal mitochondrial injury and apoptosis through suppression of Drp-1 translocation. *J Nephrol.* 2013;26(6):1073-1082.
28. Ge Y, Zhang R, Feng Y, Li H. Mbd2 mediates retinal cell apoptosis by targeting the lncRNA Mbd2-AL1/miR-188-3p/Traf3 Axis in ischemia/reperfusion injury. *Mol Ther Nucleic Acids.* 2020;19:1250-1265.
29. Zager RA, Burkhart K. Myoglobin toxicity in proximal human kidney cells: roles of Fe, Ca<sup>2+</sup>, H<sub>2</sub>O<sub>2</sub>, and terminal mitochondrial electron transport. *Kidney Int.* 1997;51(3):728-738.
30. Yang R, Xu X, Li H, et al. p53 induces miR199a-3p to suppress SOCS7 for STAT3 activation and renal fibrosis in UUO. *Sci Rep.* 2017;7:43409.
31. Zhang D, Pan J, Xiang X, et al. Protein kinase C $\delta$  suppresses autophagy to induce kidney cell apoptosis in cisplatin nephrotoxicity. *J Am Soc Nephrol.* 2017;28(4):1131-1144.
32. Hedrich CM, Crispin JC, Rauen T, et al. cAMP response element modulator alpha controls IL2 and IL17A expression during CD4 lineage commitment and subset distribution in lupus. *Proc Natl Acad Sci USA.* 2012;109(41):16606-16611.
33. Wang J, Pan J, Li H, et al. lncRNA ZEB1-AS1 was suppressed by p53 for renal fibrosis in diabetic nephropathy. *Mol Ther Nucleic Acids.* 2018;12:741-750.
34. Xu X, Pan J, Li H, et al. Atg7 mediates renal tubular cell apoptosis in vancomycin nephrotoxicity through activation of PKC- $\delta$ . *FASEB J.* 2019;33(3):4513-4524.
35. Wu D, Chen X, Guo D, et al. Knockdown of fibronectin induces mitochondria-dependent apoptosis in rat mesangial cells. *J Am Soc Nephrol.* 2005;16(3):646-657.
36. Alvarado S, Wyglinski J, Suderman M, Andrews SA, Szyf M. Methylated DNA binding domain protein 2 (MBD2) coordinately silences gene expression through activation of the microRNA hsa-mir-496 promoter in breast cancer cell line. *PLoS One.* 2013;8:e74009.
37. Klug M, Rehli M. Functional analysis of promoter CpG methylation using a CpG-free luciferase reporter vector. *Epigenetics.* 2006;1(3):127-130.

**How to cite this article:** Sun T, Liu Q, Wang Y, Deng Y, Zhang D. MBD2 mediates renal cell apoptosis via activation of Tox4 during rhabdomyolysis-induced acute kidney injury. *J Cell Mol Med.* 2021;25:4562–4571. <https://doi.org/10.1111/jcmm.16207>